



HAL
open science

Atraumatic Insertion of a Cochlear Implant Pre-Curved Electrode Array by a Robot-Automated Alignment with the Coiling Direction of the Scala Tympani

Renato Torres, Baptiste Hochet, Hannah Daoudi, Fabienne Carré, Isabelle Mosnier, Olivier Sterkers, Evelyne Ferrary, Yann Nguyen

► **To cite this version:**

Renato Torres, Baptiste Hochet, Hannah Daoudi, Fabienne Carré, Isabelle Mosnier, et al.. Atraumatic Insertion of a Cochlear Implant Pre-Curved Electrode Array by a Robot-Automated Alignment with the Coiling Direction of the Scala Tympani. *Audiology and Neurotology*, 2021, pp.1 - 8. 10.1159/000517398 . hal-03294163

HAL Id: hal-03294163

<https://hal.sorbonne-universite.fr/hal-03294163>

Submitted on 21 Jul 2021

HAL is a multi-disciplinary open access archive for the deposit and dissemination of scientific research documents, whether they are published or not. The documents may come from teaching and research institutions in France or abroad, or from public or private research centers.

L'archive ouverte pluridisciplinaire **HAL**, est destinée au dépôt et à la diffusion de documents scientifiques de niveau recherche, publiés ou non, émanant des établissements d'enseignement et de recherche français ou étrangers, des laboratoires publics ou privés.

Atraumatic Insertion of a Cochlear Implant Pre-Curved Electrode Array by a Robot-Automated Alignment with the Coiling Direction of the Scala Tympani

Renato Torres^{a, b} Baptiste Hochet^{a, c} Hannah Daoudi^{a, c} Fabienne Carré^{a, c}
Isabelle Mosnier^{a, c} Olivier Sterkers^{a, c} Evelyne Ferrary^{a, c} Yann Nguyen^{a, c}

^aTechnologies et thérapie génique pour la surdité, Institut de l'Audition, Institut Pasteur/Inserm, Paris, France;

^bDepartamento de Ciencias Fisiológicas, Facultad de Medicina, Universidad Nacional de San Agustín de Arequipa, Arequipa, Peru; ^cUnité fonctionnelle Implants auditifs et explorations fonctionnelles, Service ORL, GH Pitié-Salpêtrière, AP-HP Sorbonne Université, Paris, France

Keywords

Cochlear implants · Robot · Navigation · Cochlear/injuries · Electrodes · Implanted/adverse effects

Abstract

Introduction: Electrode array translocation is an unpredictable event with all types of arrays, even using a teleoperated robot in a clinical scenario. We aimed to compare the intracochlear trauma produced by the HiFocus™ Mid-Scala (MS) electrode array (Advanced Bionics, Valencia, CA, USA) using a teleoperated robot, with an automated robot connected to a navigation system to align the pre-curved tip of the electrode array with the coiling direction of the scala tympani (ST). **Methods:** Fifteen freshly frozen temporal bones were implanted with the MS array using the RobOtol® (Collin, Bagnoux, France). In the first group ($n = 10$), the robot was teleoperated to insert the electrode array into the basal turn of the ST under stereomicroscopic vision, and then the array was driven by a slow-speed hydraulic insertion technique with an estimated placement of the pre-curved electrode tip. In the second group ($n = 5$), 3 points were obtained from

the preoperative cone-beam computed tomography: the 2 first defining the ST insertion axis of the basal turn and a third one at the center of the ST at 270°. They provided the information to the automated system (RobOtol® connected with a navigation system) to automatically align the electrode array with the ST insertion axis and to aim the pre-curved tip toward the subsequent coiling of the ST. After this, the electrode array was manually advanced. Finally, the cochleae were obtained and fixed in a crystal resin, and the position of each electrode was determined by a micro-grinding technique. **Results:** In all cases, the electrode array was fully inserted into the cochlea and the depth of insertion was similar using both techniques. With the teleoperated robotic technique, translocations of the array were observed in 7/10 insertions (70%), but neither trauma nor array translocation occurred with automated robotic insertion. **Conclusion:** We have successfully tested an automated insertion system (robot + navigation) that could accurately align a pre-curved electrode array to the axis of the basal turn of the ST and its subsequent coiling, which reduced intracochlear insertion trauma and translocation.

© 2021 S. Karger AG, Basel

Introduction

Cochlear implants are electronic devices that can restore hearing in people with severe to profound hearing loss. This device has an internal part with an electrode array surgically implanted into the cochlea. Stimulation of the residual neurosensory auditory structures can be achieved with the implanted electrode array and hearing can be rehabilitated through these implanted devices.

Among the many factors which could affect auditory performance after cochlear implantation, intracochlear trauma induced by electrode array insertion should be limited as much as possible [Wanna et al., 2015; Kamakura and Nadol, 2016; O'Connell et al., 2016]. Previous studies have shown that preservation of intracochlear structures such as the basilar membrane or the osseous spiral lamina yields better results in terms of postoperative hearing thresholds [Finley et al., 2008; Wanna et al., 2015]. Indeed, translocation of the electrode array from the scala tympani (ST) toward the scala vestibuli (SV) remains an unpredictable and relatively common event, which could influence the hearing performance of the cochlear implant throughout the patient's life.

Although an important concern during array insertion is to decrease intracochlear trauma, previous studies have reported such deleterious events with all types of arrays [Finley et al., 2008; Boyer et al., 2015; Wanna et al., 2015; O'Connell et al., 2016; Dees et al., 2018; Riggs et al., 2019; Zelener et al., 2020; Daoudi et al., 2021; Vittoria et al., 2021]. Intracochlear trauma is associated with both decreased hearing performance in patients and loss of residual hearing in the case of hearing preservation attempts [Wanna et al., 2011]. Among the strategies used to decrease trauma, a robotic surgical approach is a viable alternative as the robot offers increased accuracy compared with manual insertion [Torres et al., 2018b]. Up to the present time, 2 robotic approaches have been developed for cochlear implantation as follows: on the one hand, robots for a minimally invasive transmastoid approach to the round window [Kratchman et al., 2011; Venail et al., 2015; Ansó et al., 2016] and on the other hand, a teleoperated robot (RobOtol[®]; Collin, Bagneux, France) to optimize electrode array insertion into the cochlea after conventional exposure of the round window [Torres et al., 2017]. Electrode array insertions are routinely performed with RobOtol[®] at very low speeds [Vittoria et al., 2021]. It was observed that translocations within the SV occurred after either manual or robotic insertions, and the frequen-

cies of these translocations differed widely according to electrode type, straight or pre-curved array, and the brand used [Daoudi et al., 2021]. Similarly, a high rate of translocations occurred with the HiFocus[™] Mid-Scala (MS) electrode array (Advance Bionics, Valence, CA, USA) regardless of whether insertion of this pre-curved array was manual or with a teleoperated robot [Daoudi et al., 2021].

To reduce the trauma of electrode array insertion, an automated system was designed by connecting the robot to a navigation device to drive the pre-curved tip of the electrode array toward the subsequent ST coiling. The experiments were conducted using the MS electrode array. Consequently, the goal of the study was to compare the intracochlear trauma produced by the pre-curved MS array using either a teleoperated robot or an automated robot connected to a navigation system to align the tip of the pre-curved array to the subsequent coiling direction of the ST.

Materials and Methods

Fifteen freshly frozen cadaveric temporal bones (TB) were obtained from the Institute of Anatomy (Centre du Don de Corps, Université Paris Descartes, Inserm CAJ-2017-078). All data were anonymously treated, and researchers have no access to the identity of the donors. People who donated their bodies voluntarily to research signed an informed consent. Ethical approval for the use of these bones is not required in this study according to the guidelines of our institute. A mastoidectomy with a posterior tympanotomy and an inferior extended round window cochleostomy were performed. The MS array loaded on its insertion tool was used for all insertions. The array is composed of 16 active electrodes with a 23.7-mm length, an active length of 15 mm, and basal and tip diameters of 0.7 and 0.5 mm, respectively. A distal blue mark indicates when the array should be ejected from the stylet by pushing the insertion tool cursor manually, with the tool still being held with the other hand.

The RobOtol[®] system (Collin, Bagneux, France) was used in 2 different ways as follows: in Group 1 ($n = 10$ TB), the RobOtol[®] was teleoperated to align the MS electrode array with the centerline axis of the basal turn of the ST according to its own estimation under microscopic magnification (Universal S2; Carl Zeiss Meditec, Oberkochen, Germany) as already reported [Torres et al., 2017], and in Group 2 ($n = 5$ TB), the robot was connected to an electromagnetic navigation system (FasTrak[®]; Polhemus, Vermont, USA) to align the electrode array with the programmed centerline of the basal turn of the ST and then to steer the pre-curved tip of the electrode array toward the coiling direction of the middle turn of the ST so that the insertion was automatically controlled.

Teleoperated Electrode Array Insertion

In Group 1, the electrode array was inserted into the ST by the teleoperated robot. Then the electrode array was ejected from the insertion tool using a syringe-driven system.

1st Step: Teleoperated Alignment and Insertion of the Electrode Array

The array was mounted on the insertion tool, specifically designed by the manufacturer, and attached to the robotic arm (shown in Fig. 1), and the TB was fixed in the surgical position by a plastic holder. Once the insertion tool was mounted on the robotic arm, the pre-curved tip of the electrode array was rotated by the surgeon to steer the array according to the optimal centerline axis of the basal turn of the ST. The optimal insertion axis was estimated by the surgeon using a mental representation of the cochlea considering the facial nerve canal [Torres et al., 2016, 2017]. Then, under the stereomicroscopic view, the surgeon teleoperated the robot driving the electrode array until it reached the first blue mark at the level of the round window.

2nd Step: Syringe-Driven Insertion of the Electrode Array

The array was then gradually inserted and ejected from the insertion tool into the cochlea by activating a Vial Medical SE 400 syringe driver (Fresenius Kabi, Bad Homburg, Germany). This syringe driver pushed a 20-mL syringe filled with saline serum connected to a second 1-mL syringe which was connected to the insertion tool. While the syringe driver progressed, the insertion tool cursor was activated by a 1-mL syringe piston. The syringe driver speed was set at 900 mL/h, yielding in an array insertion speed of $0.3 \text{ mm} \times \text{s}^{-1}$ (shown in Fig. 2).

Automated Robotic Insertion of the Electrode Array

In Group 2, the electrode array was aligned to the ST coiling. It was inserted by the automated robotic system until the blue mark was reached and then manually following the programmed positioning of the pre-curved tip of the electrode array. Four fiducial markers were screwed onto the cortical bone using a 2-mm diamond bur and preimplantation cone-beam computed tomography (CT) was performed to program the navigation of the robot and align the electrode array. The electromagnetic emitter of the tracking system was attached to the TB.

1st Step: Determination of the Insertion Axis and Coiling Direction of the ST

Preimplantation cone-beam CT was performed using an automatic protocol (Hi resolution, field of view: 8×8 , interslice interval: $0.125 \mu\text{m}$). All images were analyzed using OsiriX 4.0 (Pixmeo, Geneva, Switzerland). The distance A was measured in all specimens at the level of the basal turn (distance from the middle of the round window to the lateral wall passing by the modiolus). The cochlear duct length (CDL) at the level of the center of the cochlear duct was calculated according to the following formula: $\text{CDL (mm)} = 4.16 (A) - 4$ (A: distance A) [Alexiades et al., 2015]. Then, the optimal axis was calculated for direct access to the entry point of the cochlea as follows [Torres et al., 2018a, b]:

1. The basal turn of the cochlea was placed parallel to the coronal plane,
2. The intersection of the 3 planes was placed over the entry point to the cochlea,
3. The sagittal plane was aligned to the center of the basal turn, and the axial plane aligned to the ST,
4. A rotation of this axis was performed for direct access from the posterior tympanotomy to the entry point of the cochlea according to the position of the facial nerve canal, and



Fig. 1. Devices that allow coupling of the insertion tool to the robot. **a** Insertion tool mounted on the coupling device. **b** Coupling device attached to the FasTrak[®] emitter and the insertion tool.

5. The 3D co-ordinates of 2 points were obtained to determine the centerline axis: the first at the position of the entry point to the cochlea and the second in the center of the ST at the beginning of the coiling of the basal turn.

The 3D co-ordinates of a third point corresponding to the position of the ST at 270° were calculated to orientate the pre-curved tip of the electrode array within the ST before the electrode was ejected from the insertion tool (shown in Fig. 3).

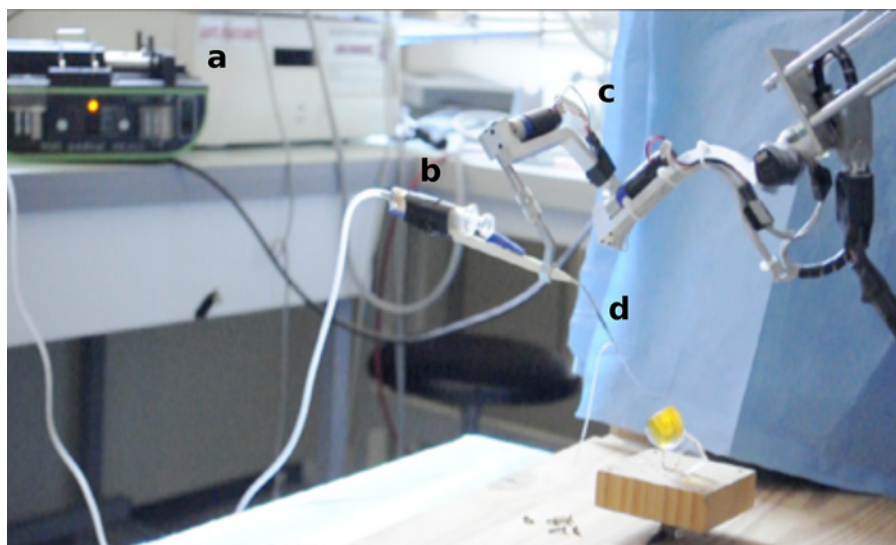
2nd Step: Navigation-Guided Robotic Alignment

The arm of the robot was automatically controlled according to the co-ordinates of the 3 selected points obtained from the preimplantation cone-beam CT:

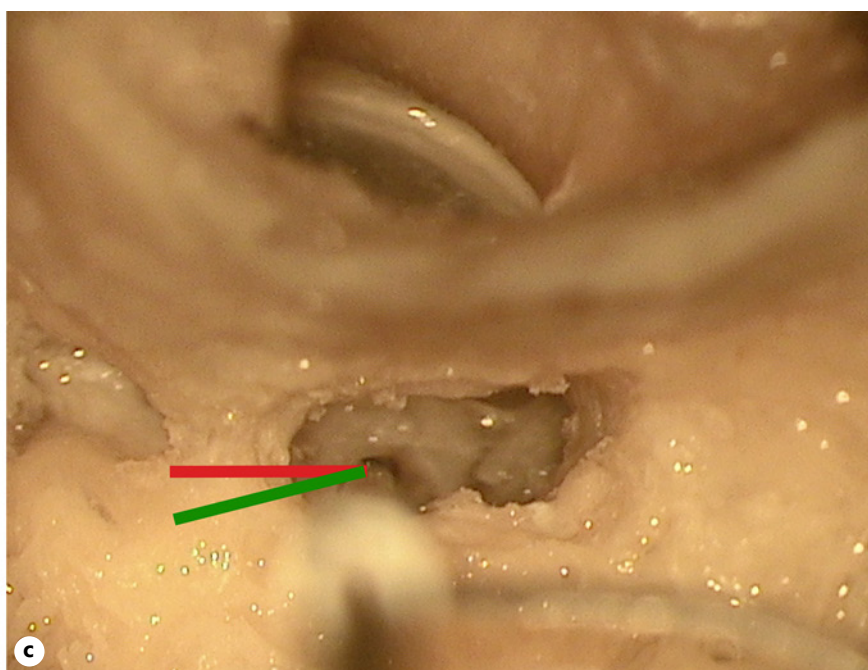
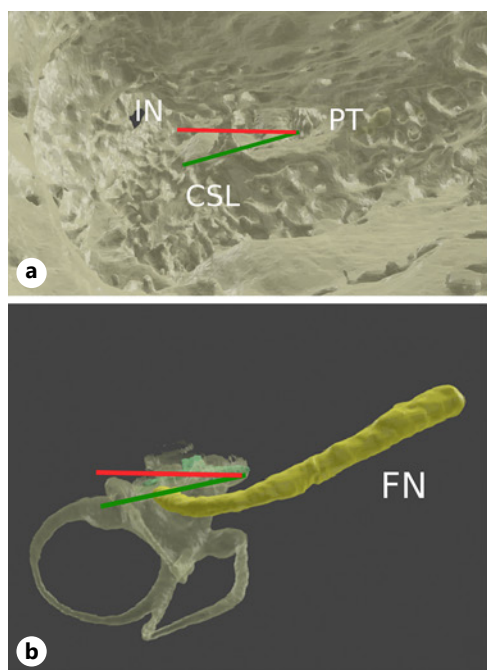
1. The entry point to the cochlea
2. The beginning of the coiling of the basal turn of the cochlea
3. The position of the ST at 270°

FasTrak[®] was used to determine the position of the robotic arm in relation to the TB and was controlled by in-house software. Electromagnetic emitters were attached to both the insertion tool and the TB. Once the tool had been attached to the robotic arm, the position of the array was calibrated as a function of the position of the TB. The 4 fiducial markers were used to calibrate the position

Fig. 2. Syringe-driven insertion. The system is composed of 2 syringes: a 20-mL syringe on the syringe driver (a) and a 1-mL syringe on the insertion tool connected to the venous infusion tubing filled with saline serum (b). The syringe driver pushes the 20-mL syringe that will in turn push the 1-mL syringe piston and the cursor from the array insertion tool. The syringe drive speed was 900 mL/h resulting in a $0.3\text{-mm} \times \text{s}^{-1}$ array insertion speed. Robotic arm (c), and electrode array (d).



Color version available online



Color version available online

Fig. 3. Comparison between the axis of the posterior tympanotomy and the coiling direction of the ST. **a** Surface image of a 3D reconstruction of a TB; the red line is parallel to the posterior tympanotomy, the green line corresponds to the coiling direction of the ST. **b** At the same level as **a**, the bone was subtracted and the green line follows the direction of the ST. **c** Surgical visualization of the same TB. IN, incus; CSL, lateral semicircular canal; PT, posterior tympanotomy; FN, facial nerve; TB, temporal bone; ST, scala tympani.

of the TB according to their positions on the preoperative cone-beam CT. The position of the array was determined with the Fas-Trak tool by recording the position of the tip of the array, the position of the 4 points surrounding the array at the level of the second blue mark used to define the position of the center of the array, and a final point indicating the direction where the array bends when ejected.

Once the calibration had been assessed, the surgeon activated the rotation to align the tip of the array with the direction of the ST and then to align the array with the insertion axis. Then, the rotation was locked and the electrode array moved automatically through the mastoid cavity to reach the round window and then to penetrate into the cochlea as far as the beginning of the basal turn of coiling of the ST. Once the electrode array has been auto-

matically placed according to its programmed position, it was manually ejected from the insertion tool. The insertion lasted about 20 s (average speed of $1 \text{ mm} \times \text{s}^{-1}$). Once the array insertion had been performed by either the teleoperated robot or the automated technique, and the array was fixed in position with a drop of 1% cyanoacrylate glue.

Evaluation of Intracochlear Trauma

The cochlea was removed from the TB without moving the array. The cochlea was fixed for 24 h with 10% formaldehyde and dehydrated with increasing concentrations of ethanol (50, 70, 90, and 100%, 3 h each). The specimens were mounted in crystal resin (Pebeo, Gémenos, France) until polymerization [Torres et al., 2018a]. A micro-grinding technique was used to assess the intracochlear trauma from insertion. The grinding direction was perpendicular to the round window/apex plane. The intracochlear trauma for each electrode was classified as follows [Eshraghi et al., 2015] (shown in Fig. 4):

- Grade 0: no trauma
- Grade 1: displacement of the basilar membrane
- Grade 2: basilar membrane rupture
- Grade 3: dislocation of the array into the SV
- Grade 4: dislocation of the array into the SV and spiral osseous lamina fracture

The position of each electrode was classified into 3 categories as follows: ST electrode (grade 0, 1, and 2 trauma), SV electrode (grade 3 and 4 trauma), and extracochlear electrode. The numbers of electrodes inserted into the ST and the functional cochlear coverage are reported in Table 1. The functional cochlear coverage was considered to be the ratio between the length of the cochlea in which the electrodes were placed into the ST (expressed in millimeters) and the CDL (see above, determination of the insertion axis and coiling direction of the ST section).

Statistical Analysis

Results are expressed as means \pm standard deviation. All data were analyzed using R 3.1.2 statistical software (R Core Team, Vienna, Austria). Quantitative variables were summarized by the measure of central tendency. Nonparametric tests were used to determine differences between the 2 insertion techniques. A p value <0.05 was considered to be statistically significant.

Results

Anatomic Characteristics

The distance A and CDL were similar in both groups (Table 1). There was no significant difference between groups on the coiling direction of the ST according to the plane of the facial canal at the level of the posterior tympanotomy (automatic group: $22 \pm 7.5^\circ$ and manual: $17 \pm 8.3^\circ$).

Teleoperated Versus Automated Alignment Technique

The electrode array was fully inserted independently of the insertion technique (shown in Fig. 5). The depth

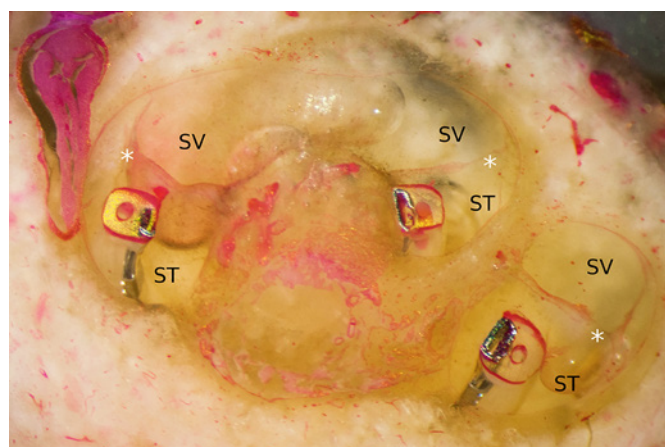


Fig. 4. Photograph of the cochlea after array insertion. The micro-grinding technique allowed the intracochlear trauma to be assessed at the level of each electrode after the Mid-Scala array insertion. ST, scala tympani; SV, scala vestibuli; white asterisk, basilar membrane.

of insertion was not different between the 2 groups (Table 1). We observed a significant decrease of translocations, from 70% of translocation in the teleoperated alignment group ($n = 10$) to none in the automated robotic technique ($n = 5$) ($p = 0.04$, χ^2 test). A single case of a slight displacement of the basilar membrane was observed in the automated robotic group (shown in Fig. 5). All translocations of the electrode array occurred around 180° ($190 \pm 33.1^\circ$). The number of electrodes inserted into the ST was higher using the automatic insertion technique than with the manual technique ($p = 0.02$, Mann-Whitney U test). There was a trend toward an increased functional cochlear coverage with the automatic insertion technique, although this was not significant ($p = 0.07$, Mann-Whitney U test) (Table 1).

Discussion

Previous studies have shown that the insertion axis of the ST into the first portion of the basal turn of the cochlea was an important factor to reduce intracochlear trauma during array insertion [Torres et al., 2018a, b]. An advantage of the MS array is the presence of an insertion tool with a system to eject the electrode array when its distal pre-curved extremity has reached $80\text{--}90^\circ$ as indicated by a blue mark on the electrode.

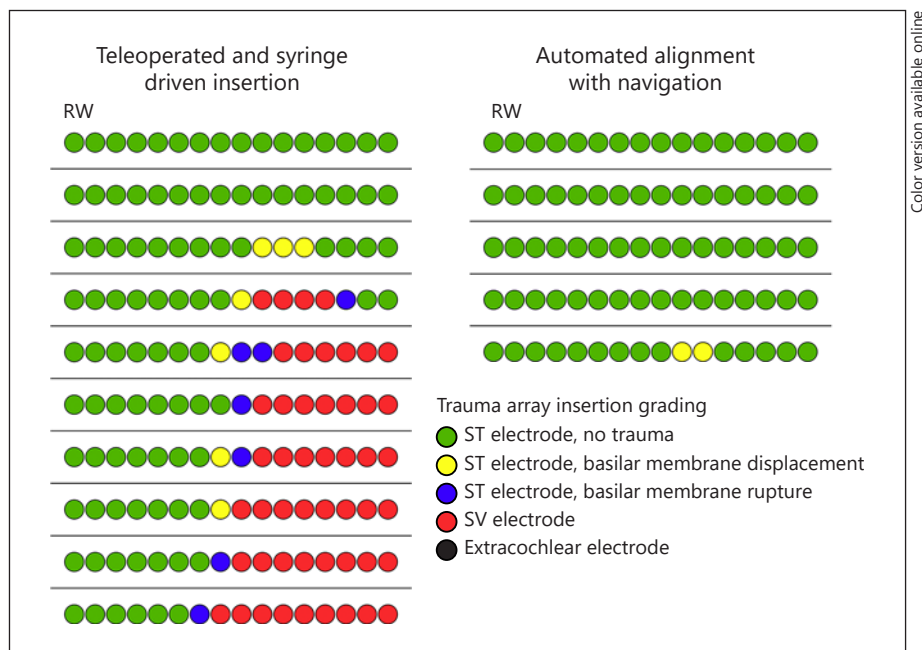
Consistent with the notion that the electrode array should be inserted in an atraumatic fashion, the MS array

Table 1. Comparison of pre- and post-insertion factors for the automated and teleoperated alignment of the MS electrode array

	Automated (<i>n</i> = 5) (X ± SD)	Teleoperated (<i>n</i> = 10) (X ± SD)	<i>p</i> value ¹
Distance A, mm	9.2±0.43	9±0.23	0.29
CDL, mm	34.3±1.79	33.3±0.94	0.29
Depth of insertion, degrees	425±28.6	413±25.0	0.42
Electrodes (N) inserted into ST	16±0.0	11±3.6	0.02*
Functional cochlear coverage, %	45±2.3	33±9.7	0.07

MS, Mid-Scala; SD, standard deviation; CDL, cochlear duct length; ST, scala tympani.
* *p* < 0.05. ¹ Mann-Whitney U test. ST: scala tympani.

Fig. 5. Comparison of the intracochlear trauma produced with the teleoperated robot and the automated robotic systems for alignment of the electrode array. ST, scala tympani; SV, scala vestibuli; RW, round window.



was coupled to the RobOtol[®], which is used to perform ear and cochlear implant surgery in patients [Daoudi et al., 2021; Vittoria et al., 2021]. However, in those clinical studies, insertions were performed at low speed but without control of the position of the pre-curved tip. To go further, we coupled the RobOtol[®] with a navigation system in order to automatically align the electrode array with the insertion axis of the ST and place the pre-curved tip in the direction of the coiling of the ST. In agreement with previous reports, a personalization of the surgery allowed to reduce the intracochlear trauma. A previous report considered the entry point to the cochlea, the entry vector, and the depth of the curling of the cochlea [Labadie et al., 2018]. Even though all instructions were written and insertions were manually performed, there was a reduction to the intracochlear trauma. Other study considered the geometry of the array and the size of the

cochlea, and the insertion was performed automatically by a mini-invasive access to the cochlea, the intracochlear trauma being significantly diminished [Rau et al., 2015]. Although the benefits of a personalization of the array insertion are obvious, the use of a surgical robot coupled with navigation and the automatization of the procedure could be a requirement to perform a personalized surgery.

Our data showed a higher rate of electrode translocations than in the previous studies reported in humans (3–34%) [Wanna et al., 2014; Boyer et al., 2015; O’Connell et al., 2016; Daoudi et al., 2021]. This difference may be accounted for by the freshly frozen TB preparations which differ significantly from living tissue. Furthermore, in the previous studies, electrode translocations were suspected radiologically [Wanna et al., 2014; Boyer et al., 2015; O’Connell et al., 2016], although this was an-

alyzed histologically in the present study. Electrode translocations detected using a 3D reconstruction model, which, in the previous studies, were well correlated with histologic analysis in TB [Torres et al., 2017], were found to occur similarly with the MS electrode array, but not with other arrays, whether insertion was performed manually or using the electrode mounted on RobOtol[®] [Daoudi et al., 2021]. Therefore, for the MS array, the critical factor influencing electrode translocation occurred after the electrode had been ejected from the insertion tool. No improvement was achieved when using a low speed and a stabilized syringe driver system. This suggests that the positioning of the electrode tip is crucial to avoid a translocation into the SV which might account for the lack of benefit of a controlled speed insertion in specimens on the one hand and of either manual or robotic insertion in patients on the other hand [Daoudi et al., 2021].

At variance with the above, no intracochlear trauma was observed when the electrode array was inserted using an automated robotic technique, although the post-ejection electrode progression was performed manually. The automated robotic technique, with coupling of RobOtol[®] to a navigation system, achieved not only alignment to the optimal axis of the basal turn of the ST but also placed the pre-curved tip of the electrode array in the direction of coiling of the ST. These results emphasize the importance of following the optimal insertion axis of the ST, not only in its basal turn but also in its subsequent coiled direction. On the other hand, if the tip of the MS array is not orientated toward the middle turn of the ST when the electrode is ejected from the insertion tool, it will damage the basilar membrane during its progression with a high risk of translocation into the SV.

Indeed, the robot which was programmed to automatically align the array considering 3 points (at the round window niche, at the position of the ST at 90°, and at the position of the ST at 270°) provided the alignment of the array with successively the optimal axis of the basal turn and the coiling direction of the ST. Using the present navigation system, the occurrence of intracochlear trauma would be reduced by providing correct positioning of the pre-curved array tip during the whole insertion process. To achieve high accuracy with the electromagnetic system coupled to the RobOtol[®], 4 fiducial markers should be screwed onto the TB, a serious limitation for further clinical application of this automated cochlear implantation system.

The strength of this study is that it demonstrated a dramatic reduction in intracochlear trauma compared to using the teleoperated robotic insertion. The automatic robotic system successively aligns the electrode array with the insertion axis and the coiling direction of the ST. This study has a limitation which is that the automatic robotic insertion technique was only studied using the MS array. This is because it was the only electrode array whereby both techniques studied here could use the same insertion tool and because its pre-curved extremity allowed the direction of the array to be programmed during the ejection. Further studies are required to adapt this technique to other electrode types.

In conclusion, with a programmed alignment to the centerline axis of the basal turn of the ST and the coiling direction of the ST, the HiFocusTM MS electrode array could be inserted without observable macroscopic intracochlear trauma by the automated robotic insertion technique used in this study. The orientation of the electrode array tip toward the middle turn of the ST could presumably be a critical step to reduce the rate of electrode translocations using a pre-curved electrode array, and this could be achieved by coupling a robot to a navigation system.

Acknowledgements

We thank Advanced Bionics for providing the arrays used in this work and Jean-Loup Bensimon, MD, who performed the cone-beam CT imaging necessary to program the robot.

Statement of Ethics

Fifteen freshly frozen cadaveric TBs were obtained from the Institute of Anatomy (Centre du Don de Corps, Université Paris Descartes, Inserm CAJ-2017-078). All data were anonymously treated, and researchers have no access to the identity of the donors. People who donated their bodies voluntarily to research signed an informed consent. Ethical approval for the use of these bones is not required in this study according to the guidelines of our institute. All data were anonymously treated, and researchers had no access to the identity of donors (Centre du Don de Corps, Université Paris Descartes, Inserm CAJ-2017-078).

Conflict of Interest Statement

The authors have no conflicts of interest to declare. Olivier Sterkers is a member of the Editorial Board of *Audiology & Neurotology*.

Funding Sources

The study was supported by research funding from the Agir pour l'Audition Foundation (Starting Grant IDA-2020), ANR Robocop ANR-19-CE19-0026-02.

Author Contributions

Renato Torres: conception, acquisition, analysis, interpretation of data, and drafting the work. Baptiste Hochet: acquisition, analysis, and interpretation of data. Hannah Daoudi, Fabienne Carré, and Isabelle Mosnier: analysis and interpretation of data. Olivier Sterkers: interpretation of data, revision, and final approval of the manuscript. Evelyne Ferrary: conception, analysis and interpretation of data, and revision of the manuscript. Yann Nguyen: conception, interpretation of data, and revision of the manuscript.

References

- Alexiades G, Dhanasingh A, Jolly C. Method to estimate the complete and two-turn cochlear duct length. *Otol Neurotol*. 2015 Jun;36(5):904–7.
- Ansó J, Dür C, Gavaghan K, Rohrbach H, Gerber N, Williamson T, et al. A neuromonitoring approach to facial nerve preservation during image-guided robotic cochlear implantation. *Otol Neurotol*. 2016 Jan;37(1):89–98.
- Boyer E, Karkas A, Attye A, Lefournier V, Escude B, Schmerber S. Scalar localization by cone-beam computed tomography of cochlear implant carriers: a comparative study between straight and periomodiolar precurved electrode arrays. *Otol Neurotol*. 2015 Mar;36(3):422–9.
- Daoudi H, Lahlou G, Torres R, Sterkers O, Lefeuve V, Ferrary E, et al. Robot-assisted cochlear implant electrode array insertion in adults: a comparative study with manual insertion. *Otol Neurotol*. 2021 Apr;42(4):e438–44.
- Dees G, Smits JJ, Janssen AML, Hof JR, Gazibegovic D, Hoof MV, et al. A mid-scala cochlear implant electrode design achieves a stable post-surgical position in the Cochlea of patients over time—a Prospective Observational Study. *Otol Neurotol*. 2018 Apr;39(4):e231–9.
- Eshraghi AA, Lang DM, Roell J, Van De Water TR, Garnham C, Rodrigues H, et al. Mechanisms of programmed cell death signaling in hair cells and support cells post-electrode insertion trauma. *Acta Otolaryngol*. 2015 Apr;135(4):328–34.
- Finley CC, Holden TA, Holden LK, Whiting BR, Chole RA, Neely GJ, et al. Role of electrode placement as a contributor to variability in cochlear implant outcomes. *Otol Neurotol*. 2008 Oct;29(7):920–8.
- Kamakura T, Nadol JB. Correlation between word recognition score and intracochlear new bone and fibrous tissue after cochlear implantation in the human. *Hear Res*. 2016 Sep;339:132–41.
- Kratchman LB, Blachon GS, Withrow TJ, Balachandran R, Labadie RF, Webster RJ. Design of a bone-attached parallel robot for percutaneous cochlear implantation. *IEEE Trans Biomed Eng*. 2011 Oct;58(10):2904–10.
- Labadie RF, Noble JH. Preliminary results with image-guided cochlear implant insertion techniques. *Otol Neurotol*. 2018 Aug;39(7):922–8.
- O'Connell BP, Cakir A, Hunter JB, Francis DO, Noble JH, Labadie RF, et al. Electrode location and angular insertion depth are predictors of audiologic outcomes in cochlear implantation. *Otol Neurotol*. 2016 Sep;37(8):1016–23.
- Rau TS, Lenarz T, Majdani O. Individual optimization of the insertion of a preformed cochlear implant electrode array. *Int J Otolaryngol*. 2015 Sep2015;2015:724703.
- Riggs WJ, Dwyer RT, Holder JT, Mattingly JK, Ortmann A, Noble JH, et al. Intracochlear electrocochleography: influence of scalar position of the cochlear implant electrode on postinsertion results. *Otol Neurotol*. 2019 Jun;40(5):e503–10.
- Torres R, Drouillard M, De Seta D, Bensimon JL, Ferrary E, Sterkers O, et al. Cochlear implant insertion axis into the basal turn: a critical factor in electrode array translocation. *Otol Neurotol*. 2018a Feb;39(2):168–76.
- Torres R, Jia H, Drouillard M, Bensimon JL, Sterkers O, Ferrary E, et al. An optimized robot-based technique for cochlear implantation to reduce array insertion trauma. *Otolaryngol Head Neck Surg*. 2018b Nov;159(5):900–7.
- Torres R, Kazmitcheff G, Bernardeschi D, De Seta D, Bensimon JL, Ferrary E, et al. Variability of the mental representation of the cochlear anatomy during cochlear implantation. *Eur Arch Otorhinolaryngol*. 2016 Aug;273(8):2009–18.
- Torres R, Kazmitcheff G, De Seta D, Ferrary E, Sterkers O, Nguyen Y. Improvement of the insertion axis for cochlear implantation with a robot-based system. *Eur Arch Otorhinolaryngol*. 2017 Feb;274(2):715–21.
- Venail F, Bell B, Akkari M, Wimmer W, Williamson T, Gerber N, et al. Manual electrode array insertion through a robot-assisted minimal invasive cochleostomy: feasibility and comparison of two different electrode array subtypes. *Otol Neurotol*. 2015 Jul;36(6):1015–22.
- Vittoria S, Lahlou G, Torres R, Daoudi H, Mosnier I, Mazalaigue S, et al. Robot-based assistance in middle ear surgery and cochlear implantation: first clinical report. *Eur Arch Otorhinolaryngol*. 2021 Jan;278(1):77–85.
- Wanna GB, Noble JH, Carlson ML, Gifford RH, Dietrich MS, Haynes DS, et al. Impact of electrode design and surgical approach on scalar location and cochlear implant outcomes. *Laryngoscope*. 2014 Nov;124(Suppl 6):S1–7.
- Wanna GB, Noble JH, Gifford RH, Dietrich MS, Sweeney AD, Zhang D, et al. Impact of intrascalar electrode location, electrode type, and angular insertion depth on residual hearing in cochlear implant patients: preliminary results. *Otol Neurotol*. 2015 Sep;36(8):1343–8.
- Wanna GB, Noble JH, McRackan TR, Dawant BM, Dietrich MS, Watkins LD, et al. Assessment of electrode placement and audiological outcomes in bilateral cochlear implantation. *Otol Neurotol*. 2011 Apr;32(3):428–32.
- Zelener F, Majdani O, Roemer A, Lexow GJ, Giesemann A, Lenarz T, et al. Relations between scalar shift and insertion depth in human cochlear implantation. *Otol Neurotol*. 2020 Feb;41(2):178–85.